IEEE Open Journal of
Antennas and Propagation

Received 9 December 2022; revised 12 January 2023; accepted 14 January 2023. Date of publication 23 January 2023; date of current version 10 February 2023.

Digital Object Identifier 10.1109/OJAP.2023.3238721

Optically Transparent Antenna for Smart Glasses

YASUO MORIMOTO (Member, IEEE), SAM SHIU, IRENE WEI HUANG (Senior Member, IEEE), ERIC FEST, GENG YE, AND JIANG ZHU (Fellow, IEEE)

(Invited Paper)

Reality Labs, Meta Platforms, Inc., Menlo Park, CA 94025, USA

CORRESPONDING AUTHORS: Y. MORIMOTO AND J. ZHU (e-mail: yso@meta.com; jiangzhu@ieee.org)

This work was supported by Meta Platforms, Inc.

ABSTRACT The optically transparent antenna technology has been gaining attention in consumer electronic industry owing to its potential to release the antenna volume constraints in compact mobile devices. Earlier studies have been heavily focused on the transparent antenna integration to the display for smartphone applications, for example, to improve its spatial coverage of 5G mm-wave at the forehead side. To our knowledge, the application of the transparent antenna technology to smart glasses and augmented reality glasses, especially considering the constraints from the coexistence with optical features in the lens stack-up, has remained unexplored. Thus, for the first time, we suggest a feasible existence solution between antennas and the RF lossy layers in the lens stack-up, to reduce the negative impacts on antenna performances. A slot loop antenna formed by metal-mesh based transparent antenna film and metallic glass frame has been investigated. Experimental results of such an antenna on human head phantom shows a total efficiency better than −4.5 dB in 2.4 GHz band. Even though it is demonstrated through a 2.4 GHz antenna example, the same principle can be applied to any other sub-6 GHz antenna applications, i.e., LTE, WiFi, GNSS, etc.

INDEX TERMS Transparent antenna, invisible antenna, metaverse, augmented reality, virtual reality, smart glass, light control panel, metal mesh, Indium Tin Oxide, slot antenna.

I. INTRODUCTION

WE FUTURE immersive wearable computing platforms will connect people to the new experiences, from immersive education and training to the new possibilities in healthcare and the workplace, and beyond. The Augmented Reality (AR) and Virtual Reality (VR) devices are key to offer such immersive experiences. Consumer electronic industry has been heavily investing with commercial products already made available to the market from Meta (formerly Facebook), Google, Microsoft and many others. Despite the tremendous efforts from the industry, technology breakthroughs are demanded for developing the enabling technologies that are required to support the 3D virtual experiences and yet packing them into light-weighted, long-term lifetime, stylish and socially acceptable wearable form-factor devices. Specific to antennas on smart glasses, there are restrictions in enclosure on the conventional placement of antennas such as by Printed Circuit Board (PCB), Laser Direct Structuring (LDS), Flexible Printed Circuit (FPC), chip, metal plates, metal wires, etc. Therefore, the transparent antenna has been drawing attention from industry recently as one potential solution to address the antenna volume constraints and to achieve a high design freedom. Many transparent antenna research and application in consumer electronic domain have been focused on the transparent antenna and display integration for smart phone [1], [2], [3], [4], [5], [6], smart watch [7], [8], etc. Large space or high freedom of placement are desired in the design for antenna performance optimization, for example, antenna efficiency, antenna gain, bandwidth, antenna isolation, tuning capability, polarization, and so on. In particular, the implementation of transparent antenna and display integration provides an option to achieve 5G mm-wave coverage at the forehead side for the all-screen display phones [1]. Other

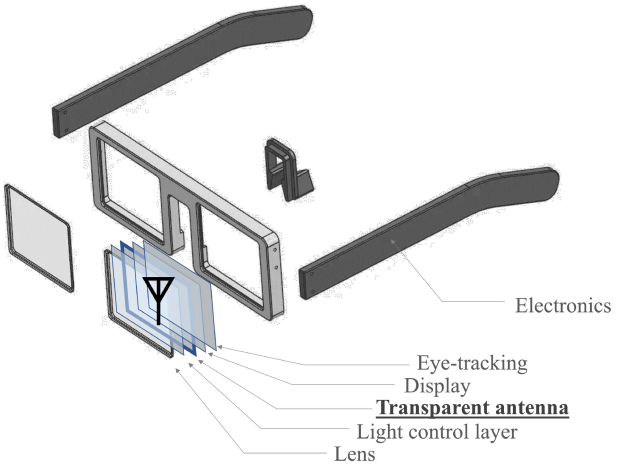

FIGURE 1. Transparent antenna and AR glass features coexistence on generic glass frame [15], [16].

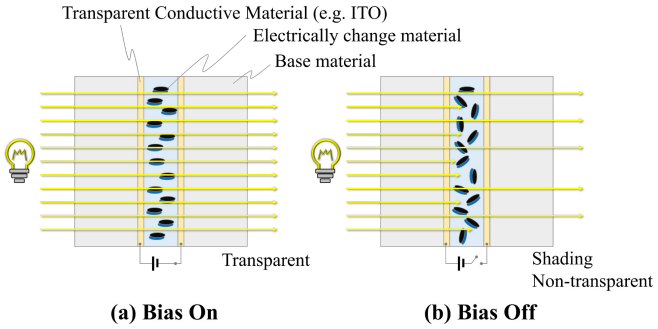

FIGURE 2. A LCL; (a) On state and (b) Off state [17], [18], [19], [20].

transparent antenna applications in the industry include but not limited to car [9], [10], solar panel [11], [12], [13], [14] applications.

Antenna design has been one of the most significant engineering challenges in hardware design for smart glasses–the antenna design is constrained by the stylish industrial design requirements, while the antenna performances suffer from severe body effects, including detuning, attenuation, and shadowing effects. From a system level, AR applications demand high throughput and low latency while the conducted power for the antenna port is constrained by the battery life requirement as well as the compliance with human electromagnetic exposure requirement, i.e., Specific Absorption Rate (SAR). On the other hand, the lenses in the glasses are the single biggest component / module in the glasses form factor, and they offer the largest real-estate in the system and the best flexibility to tune the antenna performance towards the system requirements. A generic AR glass [15], [16] is illustrated in Figure 1. Some key optical functions, i.e., micro-LED, active or passive dimming, optical waveguide, eye tracking etc., are expected to be built into the lens which help connect people from the real world to the virtual world for the immersive experiences. Hence, a major technical challenge in implementing a transparent antenna is the coordination of the transparent antenna layer with other functions that already exist in the lens stack-up. In another word, the transparent antenna must ensure the minimal optical performance degradation within acceptable range, while still demonstrating the antenna performance benefits as compared to the conventional antennas in the glasses form factors, i.e., the LDS- or the PCB-antenna in the glass temple or frame areas. While optical functional layers in the lens stack-up is still evolving with huge technical challenges in their optical performances, the Light Control Layer (LCL) is identified as the material that has the largest negative impact on antenna performances among the existing functions, and the coexistence design of lossy LCL and transparent antenna becomes key for transparent antenna to be integrated into modern smart/AR glasses.

In this paper, the LCL and transparent conductive material made by metal mesh are firstly described. Through the studies of several basic antenna types, the transparent slot antenna concept emerges to be the best option for transparent antenna to coexist with the lossy LCL. The design has been simulated and validated with prototypes.

II. TRANSPARENT MATERIALS

This section provides a review of Light Control Layer (LCL) with the analysis to explain why it has the largest negative impact on antenna. This section also reviews the typical approaches to design optical invisible but electrically conductive films.

A. LCL

The general LCL shown in Figure 2 is also known as "active dimming layer." The main types are PDLC (Polymer Dispersed Liquid Crystal) [17], [18] which is good at scatter controlled and GHLC (Guest-Host Liquid Crystal) [19], [20] which has advantages of optical transmittance controlled. In both cases, the Liquid Crystal (LC) is sandwiched between two layers of transparent conductive film (typically Indium Tin Oxide: ITO), and the orientation of the LC can be changed by applying a voltage bias, thus allowing the optical properties of the layer to be changed electrically. The choice of GHLC vs PDLC depends on the application, i.e., AR vs. VR, and also the optical features that they have to co-exist with.

At radio frequency, the ITOs on LC have significant impacts on transparent antenna performances, because of the high sheet resistivity nature of the typical ITOs. For example, the typical resistance of ITO is about 10 to 500 Ω/Sq, to maintain the acceptable optical properties. The RF impact from LC and mixed LC is minor even when the bias of LC is ON or OFF since the difference between the vertical and horizontal *Dk* and *Df* of LC is small. If a transparent antenna on lens is not designed properly, the proximity to the lossy ITOs leads to a severe performance degradation.

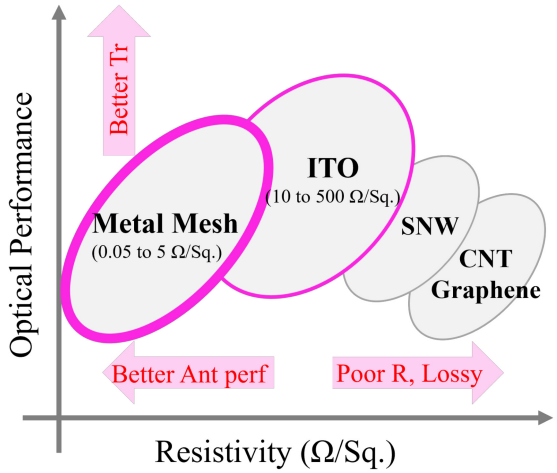

FIGURE 3. General transparent conductive material mapping shows tradeoff between transparency and resistivity.

B. TRANSPARENT CONDUCTING FILMS AND METAL MESH

Transparent conducting films (TCFs) are very thin, and the material itself is optically transparent and electrically conductive at same time. Several transparent antennas were developed using these TCFs in the past [21], [22], [23], [24], [25], [26], [27]. ITO is the most widely used TCF in electronic devices. Silver Nanowire (SNW) has randomly conducted network made by silver wires which is scaled shorter than the wavelength of visible light. Graphene and Carbon Nanotubes (CNT) are also being developed in recent years as one of the promising TCFs.

On the other hand, Metal Mesh (MM), as one of the TCFs, has been mainly used in touch sensors on display and electromagnetic shield in the past. Recently, the use of MM to design transparent antennas has gained increasing attention from the industry owing to its low resistivity [1], [2], [7], [8], [27], [28], [29], [30], [31]. MM can be made from manufacturing methods, such as subtracting method by photo-lithography, additive method by plating up, printing, transfer method, etc., these process similar to the general fine pattern for PCB or Integrated Circuit (IC) manufacturing.

Among all TCFs mentioned above, there is always a fundamental trade-off between electrical resistance and optical properties as illustrated in Figure 3. Optical properties includes the well-understood visible light transmittance as well as scattering (e.g., Haze), color parameters ($A*$, $B*$, yellowness index, etc.), and the Moire effect caused by interference with other periodic structures specific to MM. Recently, both MM and ITO based transparent films are considered for antennas. Since the MM approach provides lower resistance and more flexibility to adjust the sheet resistance vs optical transparency, the consumer industry and transparent antenna research community are both trending to use MM as the major transparent antenna materials.

The sheet resistance of MM is related to its shape, the width/thickness, the pitch of wires and metal conductivity.

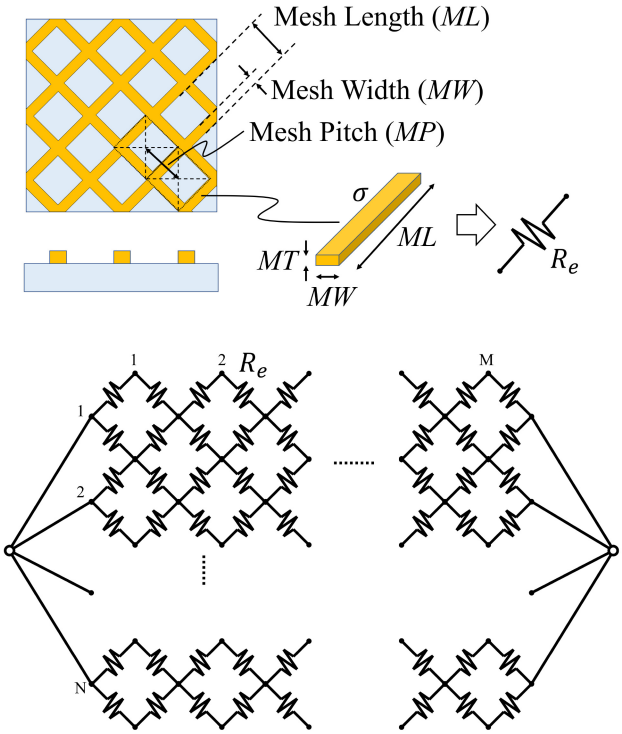

FIGURE 4. Mesh structure and resistor network schematic.

The metal mesh structure can be any geometric periodic structure, i.e., square, rectangular, hexagonal, diamond, triangular, hybrids of different shapes, rotational angles of arrangement, periodicity staggered, even randomness. In any geometric pattern, the size and periodicity of the structure is on a scale sufficiently larger than the visible light wavelength (380 nm to 780 nm). Each has its own advantages and disadvantages, from both optical and electrical perspectives. This paper describes the major parameters for the case of a 45-degree rotation of a square. Figure 4 shows the metal mesh structure and resistance network schematics.

Re is the element resistance of mesh branch, N and M is the number of mesh intersections in the width direction, and in the current path direction, respectively. The aperture ratio Ap (%), the area that one intersection can cover AC (m^2), and the DC sheet resistance Rs (Ω/Sq) can be calculated from the following equations:

$$Ap = 100\frac{(MP - MW)^2}{MP^2} \tag{1}$$

$$AC = MP^2 \tag{2}$$

$$Rs = \frac{1}{\sigma}\frac{MP}{MT \times MW} \tag{3}$$

where MW is the width, ML is the length, MP is the periodic pitch (ML and MP are the same for a squared shape), MT is the thickness, and σ is conductivity of metal mesh, respectively. The effective σ (s/m) is calculated from the measured dimensional values and DC sheet resistance Rs of the manufactured MMs. A photograph of the MMs used in this paper is given in Figure 5. MP is 200 um, MW is

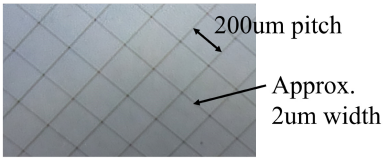

FIGURE 5. A microscope picture for metal mesh.

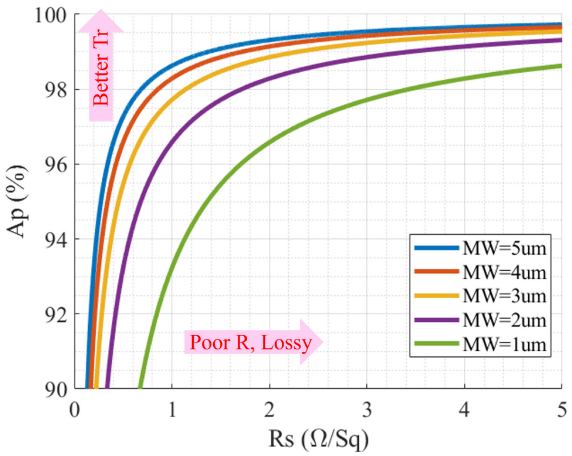

FIGURE 6. Sheet resistance Rs and aperture ratio *Ap* of metal mesh, where $MT/MW = 1.0$, $\sigma = 5.8 \times 10^7 \times 0.5$, *MP* is parameter in equation (1) and (3).

approximately 2 um, the cross sectional area multiplied by MW and MT is 2.5 um^2, and Ap is 98 (%). The measured Rs is 2 (Ω/Sq). The optical properties of metal mesh is measured by the spectrometer. The delta Tr, calibrated surface reflection, of averaged in visible light wavelength 400 to 700 nm is 97.4 (%), and of 550 nm is 97.3 (%) which are strongly correlated with Ap.

III. TRANSPARENT SLOT ANTENNA ON LCL

A. TRANSPARENT ANTENNA TYPES STUDY

A plot of calculated Ap and Rs of general configurations is given in Figure 6. The Ap based on only MP was changed to see the Rs values. The thickness of metal mesh MT has dependencies on the mesh width MW. In this calculation, we make an assumption that $MT = MW$, which is typical from the manufacturing process. The effective conductivity is set at 50% of Cu (i.e., $5.8 \times 10^7 \times 0.5$). Ap is also correlated to optical transmittance (Tr) and scattering, indicating that there is a trade-off between Rs and optical properties of metal mesh. From optical visibility perspective, it is recommended that the mesh width is no more than $2um$. From the optical transparency perspective which is correlated to AP, the wider mesh width MW, the better AP, which is indicated from Figure 6.

When it comes to antenna design, it is reminded that there are three dominant materials to form antenna elements: the transparent conductive material, e.g., metal mesh antenna layer, the lossy layer which locates in close proximity to the antenna layer, e.g., ITOs of LCL, and the metallic or plastic enclosure from the glasses. Figure 7 shows not only layer stack-up of transparent antenna and LCL on lens but also the possible antenna types that can be fit into the form factor. The actual layer stack-up should have a complicated combination of base materials and Optical Clear Adhesive (OCA) for each function. However, they're not included in this study since they're especially thin and can be negligible at radio frequency.

There are a total of five types of transparent antenna on lossy material, with Types (A) - (C) consisting of MM antenna and lossy LCL only, and Types (D)-(E) also including metal enclosures. In all types, they are multi-layer structure similar to PCBs but without vias. Type (A) is a dipole antenna. Type (B) is a Microstrip Antenna (MSA). Type (C) is a slot antenna within the transparent region. Type (D) is a monopole antenna locates at the edge of the transparent region and using metal enclosure as ground plane. Type (E) is a slot antenna formed between the transparent region and the metal enclosure. The film size of the transparent sheet is given as 40 mm by 50 mm, and its metal enclosure is a rectangular ring with a 2 mm by 2 mm cross section. In these studies, each parameter and the results of the analysis are summarized in Table 1. Except antenna size (W and L), the same materials were used in all antenna types as a fair comparison, for example, the sheet resistance of MM is 2 (Ω/Sq.), and the sheet resistances of ITOs in LCL, $Rs2$ and $Rs3$, are both 200 (Ω/Sq.). It is noted that the value of $Rs1$ on MM is determined from the target value of optical properties (e.g., Tr), and the values of H, Dk, Df, $H2$, $Dk2$, and $Df2$ are from the manufacturing process and materials. It is well understood that when the lossy ITO materials are in close proximity of the antenna, the antenna efficiency drop.

In the design of transparent antenna, the design variables include the antenna pattern, the mesh width, mesh pitch, the gap between MM layer and metal enclosure $G1$, and the gap between ITO layer and metal enclosure $G2$. The simulation results of all five types of antenna designed shown in Table 1 is described in this paragraph. All antennas are well-matched at 2.4 GHz. The radiation efficiency of Type (A) to (D) is significantly lower because the most of the RF power converts into Ohmic loss due to absorption of the resistive sheet of $Rs1$, $Rs2$, and $Rs3$. For the same reasons, it yields a large impedance matching therefore the discussion of return loss here is negligible. It is found that among all five antenna types under investigation, the type (E) edge slot antenna performs the best. In edge slot antenna design, the transparent antenna film matches the pattern of the ITO in LCL and is directly placed against the ITO layer. With such a configuration, the metal mesh layer and ITO layers are strongly coupled to each other. Majority of the currents follow the least impedance path and is distributed at the metal enclosure and the conductive metal mesh layer. The lossy effect of the ITOs can be reduced. The additional analysis with the removal $Rs2$ and $Rs3$ lossy LCL layers from Type (E) slightly improves antenna radiation efficiency from 35.88% to 38.10% indicating that the negative

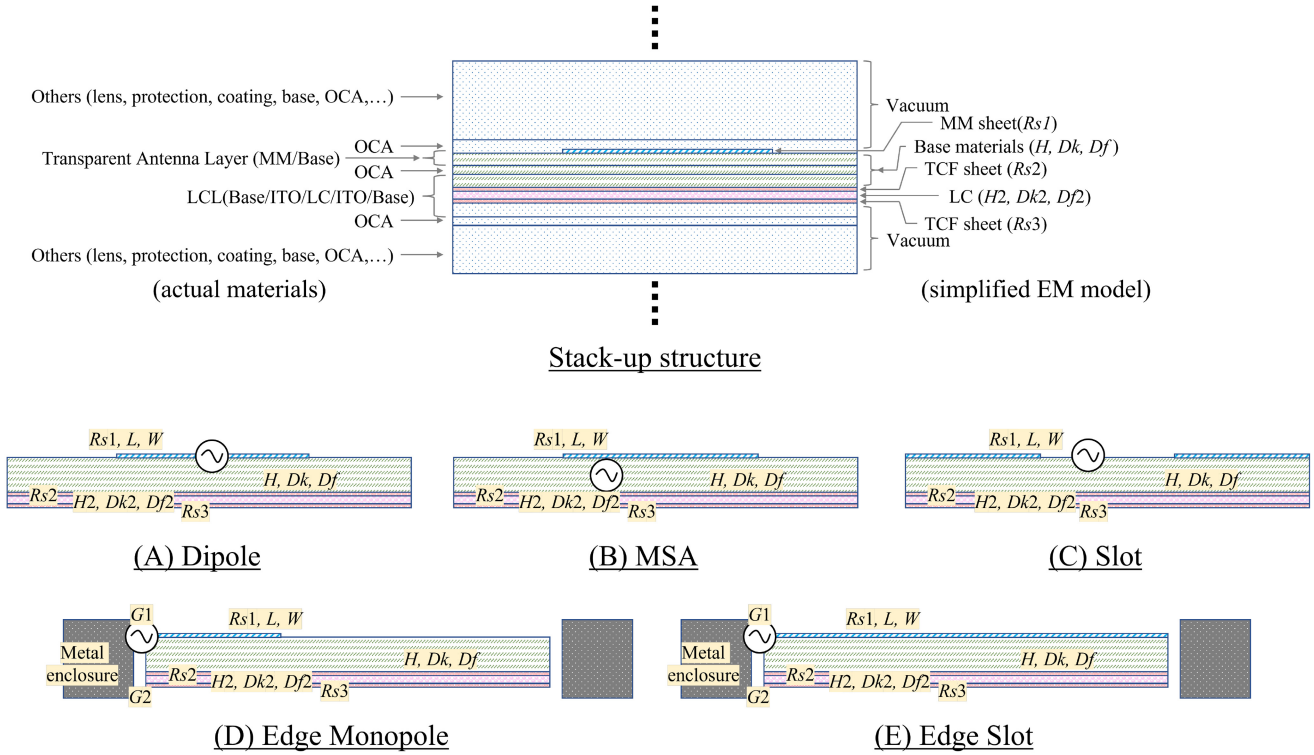

FIGURE 7. The stack-up of different type transparent antenna with lossy materials; Stack-up structure, (A) Dipole, (B) Microstrip antenna, (C) Slot antenna, (D) Edge monopole antenna, and (E) Edge slot antenna.

TABLE 1. Comparisons of different type transparent antennas with lossy materials.

Antenna type:	(A) Dipole	(B) MSA	(C) Slot	(D) Edge monopole	(E) Edge slot
			Designed parameters		
Antenna shape:	Rectangular	Square	Rectangular aperture	Rectangular	Rectangular slot loop
W, L (Antenna size):	2 mm, 25 mm	30 mm, 30 mm	0.5 mm, 30 mm	2 mm, 8 mm	40 mm, 50 mm
$Rs1$:	2 Ω/Sq.	2 Ω/Sq.	2 Ω/Sq.	2 Ω/Sq.	2 Ω/Sq.
$Rs2$:	200 Ω/Sq.	200 Ω/Sq.	200 Ω/Sq.	200 Ω/Sq.	200 Ω/Sq.
$Rs3$:	200 Ω/Sq.	200 Ω/Sq.	200 Ω/Sq.	200 Ω/Sq.	200 Ω/Sq.
H, Dk, Df :	300 um, 3.4, 0.02	300 um, 3.4, 0.02	300 um, 3.4, 0.02	300 um, 3.4, 0.02	300 um, 3.4, 0.02
$H2, Dk2, Df2$:	10 um, 3.0, 0.02	10 um, 3.0, 0.02	10 um, 3.0, 0.02	10 um, 3.0, 0.02	10 um, 3.0, 0.02
Metallic Enclosure:	No	No	No	Yes	Yes
$G1, G2$:	N/A	N/A	N/A	1 mm, 1 mm	1 mm, 1 mm
$Z0$:	50 Ω	50 Ω	50 Ω	100 Ω	25 Ω
			EM Results (2.4GHz)		
Radiated power:	4.83 %	0.01 %	3.58 %	6.30 %	35.88 %
Return loss:	6.59 %	3.10 %	5.75 %	0.75 %	3.80 %
Loss at $Rs1$ (MM, Ant):	14.55 %	1.58 %	31.40 %	4.24 %	56.08 %
Loss at $Rs2$ (TCF, LCL):	36.42 %	64.60 %	29.20 %	44.12 %	1.95 %
Loss at $Rs3$ (TCF, LCL):	36.22 %	30.26 %	29.03 %	44.02 %	2.05 %
Loss at base materials:	1.49 %	0.52 %	1.12 %	0.67 %	0.12 %
Loss at LC (LCL):	0.01 %	0.24 %	0.01 %	0.01 %	0.01 %
Loss at enclosure:	N/A	N/A	N/A	0.06 %	0.25 %

impact from LCL is minor for the proposed antenna. $G1$ and $G2$ are the key parameters to increase radiation efficiency and kept as 1 mm throughout the study. When $G1 = G2$ at Type (E) is modified up to 0.5, 1.0, 1.5, and 2.0 mm, its radiated power increases to 18.21%, 35.88%, 48.18%, and 56.44%.

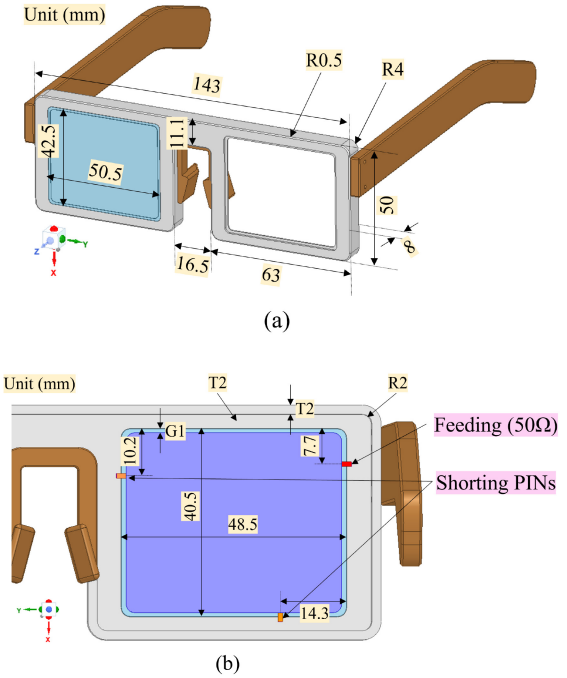

FIGURE 8. EM analysis model for (a) dimensions and (b) port/PIN locations.

B. ANTENNA CONCEPT AND DESIGN

A Type (E) antenna, i.e., edge slot antenna between transparent conductor and metallic enclosure was designed for 2.4 GHz applications. The shape of glass frame refereed from [15], [16]. For the antenna input impedance and resonance of the edge slot antenna, the tuning parameters are the locations of antenna feed and shorting PINs. Changing these parameters is equivalent to changing the length of the slot antenna or impedance match. A simulated antenna radiation pattern and current distribution are shown in Figure 9. Since the proposed edge slot antenna is slot formed between the transparent sheet (i.e., including transparent antenna layer *Rs*1, LCL transparent conductor *Rs*2, and *Rs*3) and metal enclosure, the radiation pattern radiates both to the outside and to the human side. The proposed edge slot antenna has multiple resonance including 2.16 GHz as second harmonic of a full wave length ('b' - 'A' - 'B' - 'D' - 'c') for best radiation efficiency close to 2.4GHz application, 1.6 GHz as with parasitic slot ('c' - 'C' - 'b') plus fundamental slot ('b' - 'A' - 'B' - 'D' - 'c') or, slot loop will potentially cover GPS L1 band.

The visual and representative dimensions of the model used in the analysis are shown in Figure 8. Figure 10 shows the results of the analysis of the radiation performances and reflection characteristics of the designed antenna in free space. Total efficiency of −4.40 dB, as well as excellent matching are obtained at 2.4 GHz.

IV. PROTOTYPE AND MEASUREMENT RESULTS

This chapter describes the results of the prototype evaluation for LCL and antenna performance. Figure 11 shows

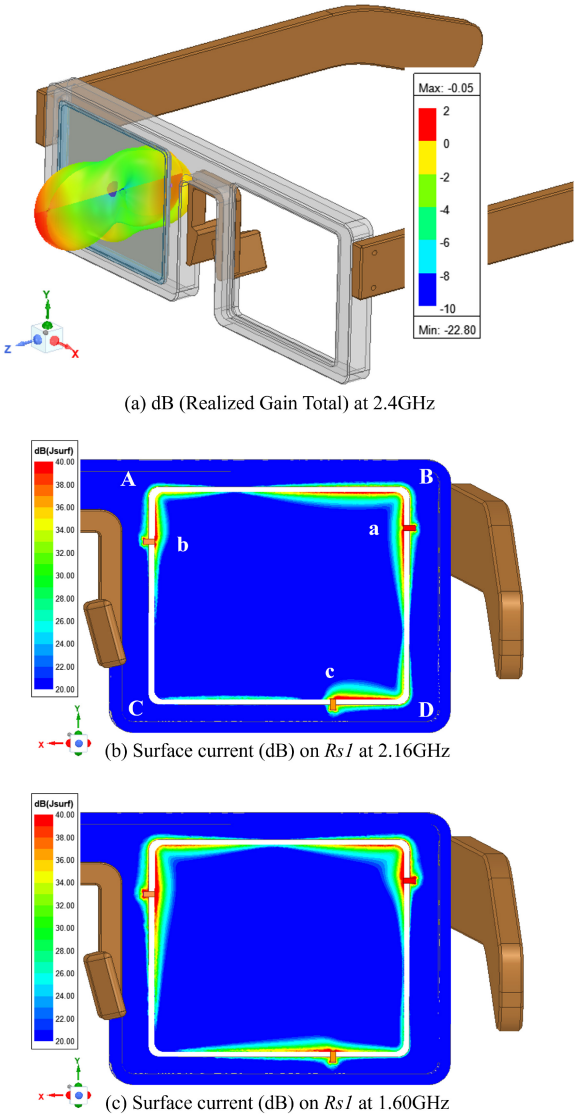

FIGURE 9. (a) simulated antenna radiation pattern at 2.4GHz, (b) surface current distribution on 2.16GHz and (c) surface current distribution on 1.6GHz, where labels for location are: 'A,' 'B,' 'C,' and 'D' as corner, 'a' as feeding, 'b' and 'c' as shorting PINs.

the prototype with one side has transparent antenna on lens and another side has lens only, both have no LCLs. The gap between MM layer and metal enclosure *G*1 and the gap between ITO layer and metal enclosure *G*2 are 1mm which is the same as the design in the previous chapter. As shown in the figure, human eyes can hardly differentiate the discrepancy between the two sides of lens.

A. LCL

LCL with PDLC was implemented in the prototype shown in Figure 12. The reason was that it was possible to correctly evaluate the relatively high loss transparent resistance that affects the antenna performance, and it is easy to fabricate. After processing and mounting the electrodes for bias,

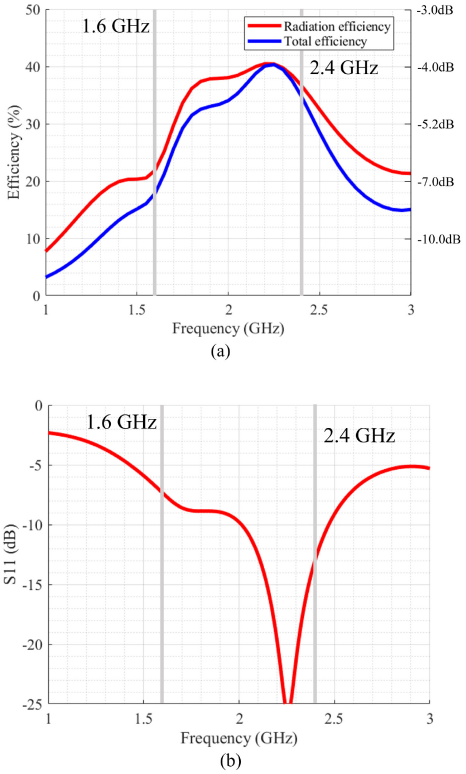

FIGURE 10. Simulated results for (a) Antenna efficiencies (b) Reflection coefficient of the proposed edge slot antenna.

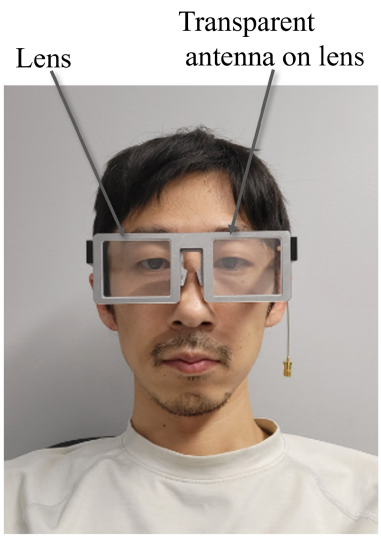

FIGURE 11. A picture of mock-up fabricated.

LCL was mounted on the lens with transparent antenna electrode. As shown in the figure, the transparency is apparently changed by turning bias ON or OFF. In additional measurement, there was almost no impact from LCL bias status on antenna performances.

B. ANTENNA

Antenna characteristics were evaluated. Figure 13 demonstrates the over-the-air measurement setup and radiated

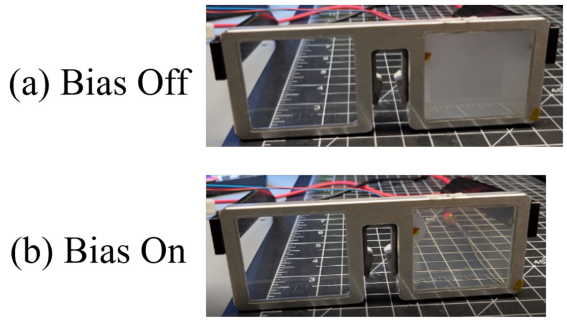

FIGURE 12. LCL test (a) Bias OFF (b) Bias ON.

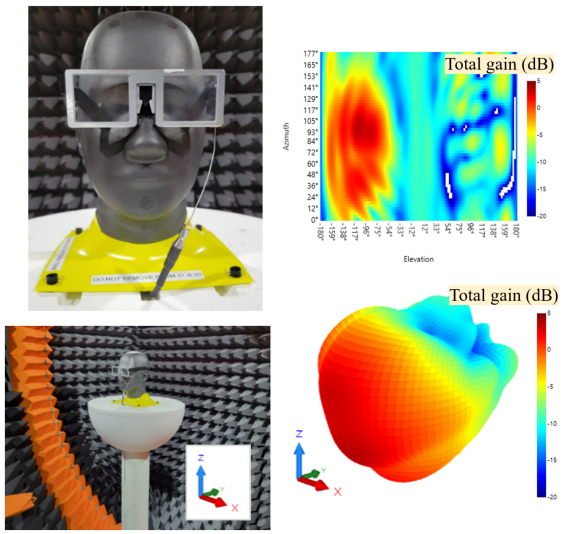

FIGURE 13. Over-the-air measurement setup and radiation pattern at 2.4GHz.

antenna pattern at 2.4 GHz. The radiation pattern indicates that the majority of the total gain shows on the world side due to the shadowing effect of the human head phantom. The measurement results of prototype with LCL are also shown Figure 14. In each of the radiation and reflection characteristics, both with and without the human head phantom were measured. A comparison of the measured results without the human head phantom and the simulated results in the previous chapter shows an excellent agreement. After taking account of 0.28 dB cable loss at 2.4 GHz, the estimated measured antenna efficiency with head phantom is −4.36 dB.

V. CONCLUSION

The transparent antenna is a good candidate to solve the antenna volume constraints for smart glasses and augmented glasses form factors. This paper summarizes the practical constraints of transparent antenna designs and performances when they co-exist with the RF lossy optical features/functions in the lens stack-up. For the first time, the edge slot antenna concept has been proposed to address the coexistence issue with the optical features, where, more

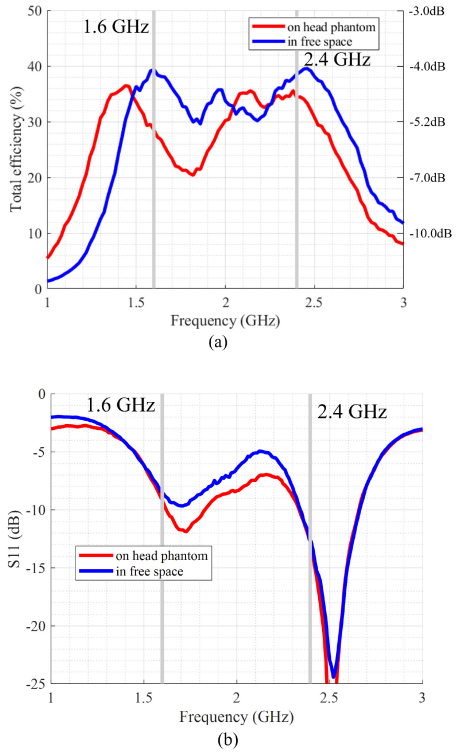

FIGURE 14. Measurement results of proposed edge slot antenna (a) antenna efficiency (b) reflection coefficient.

specifically, a matched metal mesh layer is directly attached to the lossy light control layer. With such configuration, the RF loss from the lossy optical features can be significant eliminated. Experimental results on human head phantom verified our simulation with a total efficiency of −4.36 dB at 2.4 GHz.

REFERENCES

[1] J. Park, S. Y. Lee, J. Kim, D. Park, W. Choi, and W. Hong, "An optically invisible antenna-on-display concept for millimeter-wave 5G cellular devices," *IEEE Trans. Antennas Propag.*, vol. 67, no. 5, pp. 2942–2952, May 2019.

[2] M. Kim et al., "Antenna-on-display concept on an extremely thin substrate for sub-6 GHz wireless applications," *IEEE Trans. Antennas Propag.*, vol. 70, no. 7, pp. 5929–5934, Jul. 2022.

[3] Y. Oh, J.-Y. Lee, D. Lee, D. Park, and W. Hong, "Broadband antenna-on-display applicable for WiFi," in *Proc. IEEE Int. Symp. Antennas Propag. USNC-URSI Radio Sci. Meeting (APS/URSI)*, 2021, pp. 61–62.

[4] T. D. Nguyen, K. Kim, S. R. Yoon, and G. Byun, "Optically invisible artificial magnetic conductor subarrays for triband display-integrated antennas," *IEEE Trans. Microw. Theory Techn.*, vol. 70, no. 8, pp. 3975–3986, Aug. 2022.

[5] M. Stanley, Y. Huang, H. Wang, H. Zhou, A. Alieldin, and S. Joseph, "A transparent dual-polarized antenna array for 5G smartphone applications," in *Proc. IEEE Int. Symp. Antennas Propag. USNC/URSI Nat. Radio Sci. Meeting*, 2018, pp. 635–636.

[6] S. Foo and W. Tong, "AMOLED in-display antennas," in *Proc. 14th Eur. Conf. Antennas Propag. (EuCAP)*, 2020, pp. 1–5.

[7] W. Hong, S. Ko, Y. G. Kim, and S. Lim, "Invisible antennas using mesoscale conductive polymer wires embedded within OLED displays," in *Proc. 11th Eur. Conf. Antennas Propag. (EUCAP)*, 2017, pp. 2809–2811.

[8] W. Hong, S. Lim, S. Ko, and Y. G. Kim, "Optically invisible antenna integrated within an OLED touch display panel for IoT applications," *IEEE Trans. Antennas Propag.*, vol. 65, no. 7, pp. 3750–3755, Jul. 2017.

[9] J. P. Lombardi et al., "Copper transparent antennas on flexible glass by subtractive and semi-additive fabrication for automotive applications," in *Proc. IEEE 68th Electron. Compon. Technol. Conf. (ECTC)*, 2018, pp. 2107–2115.

[10] O. Kagaya, Y. Morimoto, T. Motegi, and M. Inomata, "Transparent glass quartz antennas on the windows of 5G-millimeter-wave-connected cars," *IEICE Trans. Commun.*, vol. 104, no. 1, pp. 64–72, 2021.

[11] T. Yekan and R. Baktur, "Conformal integrated solar panel antennas: Two effective integration methods of antennas with solar cells," *IEEE Antennas Propag. Mag.*, vol. 59, no. 2, pp. 69–78, Apr. 2017.

[12] F. Nashad, S. Foti, D. Smith, M. Elsdon, and O. Yurduseven, "Development of transparent patch antenna element integrated with solar cells for Ku-band satellite applications," in *Proc. Loughborough Antennas Propag. Conf. (LAPC)*, 2016, pp. 1–5.

[13] S. Zarbakhsh, M. Akbari, M. Farahani, A. Ghayekhloo, T. A. Denidni, and A.-R. Sebak, "Optically transparent subarray antenna based on solar panel for CubeSat application," *IEEE Trans. Antennas Propag.*, vol. 68, no. 1, pp. 319–328, Jan. 2020.

[14] X. Liu, D. R. Jackson, E. Ingram, J. Chen, and M. H. Seko, "Transparent microstrip antennas for CubeSats," in *Proc. IEEE Int. Symp. Antennas Propag. USNC-URSI Radio Sci. Meeting*, 2019, pp. 845–846.

[15] Y.-Y. Wang, Y.-L. Ban, Z. Nie, and C.-Y.-D. Sim, "Dual-loop antenna for 4G LTE MIMO smart glasses applications," *IEEE Antennas Wireless Propag. Lett.*, vol. 18, pp. 1818–1822, 2019.

[16] Y.-Y. Wang, Y.-L. Ban, and Y. Liu, "Sub-6GHz 4G/5G conformal glasses antennas," *IEEE Access*, vol. 7, pp. 182027–182036, 2019.

[17] J. Xu et al., "Study on the preparation and performance of an electrically controlled dimming film with wide working temperature range," *J. Mol. Liquids*, vol. 367, Dec. 2022, Art. no. 120408.

[18] L. Chen, Y. Yang, X. Xia, M. Ju, and Z. Wu, "Design of intelligent dimming glass system," *World Sci. Res. J.*, vol. 4, no. 4, pp. 9–15, 2018.

[19] J. Kim, S.-W. Oh, J. Choi, S. Park, and W. Kim, "Optical see-through head-mounted display including transmittance-variable display for high visibility," *J. Inf. Display*, vol. 23, no. 2, pp. 121–127, 2022.

[20] J. Lee, S. Nam, and S. S. Choi, "Design of chiral guest-host liquid crystals for a transmittance-tunable smart window," *Opt. Mater. Exp.*, vol. 12, no. 7, pp. 2568–2583, 2022.

[21] H. J. Song, T. Y. Hsu, D. F. Sievenpiper, H. P. Hsu, J. Schaffner, and E. Yasan, "A method for improving the efficiency of transparent film antennas," *IEEE Antennas Wireless Propag. Lett.*, vol. 7, pp. 753–756, 2008.

[22] Y. Koga and M. Kai, "A transparent double folded loop antenna for IoT applications," in *Proc. IEEE-APS Topical Conf. Antennas Propag. Wireless Commun. (APWC)*, 2018, pp. 762–765.

[23] S. Hakimi, S. K. A. Rahim, M. Abedian, S. Noghabaei, and M. Khalily, "CPW-fed transparent antenna for extended ultrawideband applications," *IEEE Antennas Wireless Propag. Lett.*, vol. 13, pp. 1251–1254, 2014.

[24] N. Guan, H. Furuya, K. Himeno, K. Goto, and K. Ito, "Basic study on an antenna made of a transparent conductive film," *IEICE Trans. Commun.*, vol. E90-B, no. 9, pp. 2219–2224, 2007.

[25] M. R. Haraty, M. Naser-Moghadasi, A. A. Lotfi-Neyestanak, and A. Nikfarjam, "Improving the efficiency of transparent antenna using gold nanolayer deposition," *IEEE Antennas Wireless Propag. Lett.*, vol. 15, pp. 4–7, 2015.

[26] W. Li, A. Meredov, and A. Shamim, "Silver nanowire based flexible, transparent, wideband antenna for 5G band application," in *Proc. IEEE Int. Symp. Antennas Propag. USNC-URSI Radio Sci. Meeting*, 2019, pp. 275–276.

[27] S. Hong, Y. Kim, and C. W. Jung, "Transparent microstrip patch antennas with multilayer and metal-mesh films," *IEEE Antennas Wireless Propag. Lett.*, vol. 16, pp. 772–775, 2016.

[28] Y. Zhang, S. Shen, C.-Y. Chiu, and R. Murch, "A broadband transparent antenna integrated with an indoor solar cell for WLAN applications," in *Proc. IEEE Int. Symp. Antennas Propag. North Amer. Radio Sci. Meeting*, 2020, pp. 437–438.

[29] Y. Zhang, S. Shen, C.-Y. Chiu, and R. D. Murch, "A dual-band transparent coplanar patch antenna for WLAN systems," in *Proc. IEEE Int. Symp. Antennas Propag. USNC/URSI Nat. Radio Sci. Meeting*, 2018, pp. 465–466.

[30] H. J. Song et al., "Roll-to-roll printed transparent applique antennas," in *Proc. IEEE Int. Symp. Antennas Propag. USNC/URSI Nat. Radio Sci. Meeting*, 2018, pp. 1671–1672.
[31] S. H. Kang and C. W. Jung, "Transparent patch antenna using metal mesh," *IEEE Trans. Antennas Propag.*, vol. 66, no. 4, pp. 2095–2100, Apr. 2018.

YASUO MORIMOTO (Member, IEEE) received the B.E. degree in information science and engineering and the M.E. and D.E. degrees in science and engineering from Ritsumeikan University, Kyoto, Japan, in 2008, 2010, and 2019, respectively.

From 2010 to 2019, he was a Researcher with Mitsubishi Electric Corporation, Kamakura, Japan, where he was involved in the research and development of antenna feedings, microwave circuits, and RF implementations for antennas. He was a Visiting Scholar with the University of California at Los Angeles, Los Angeles, CA, USA, in 2016. From 2019 to 2021, he was a Principal Researcher/Manager with AGC Inc., Yokohama, Japan, where he was engaged in the research of antennas for radar and radio communication systems using new materials. In 2021, he joined Meta Reality Labs, Sunnyvale, CA, USA, as an Antenna Research Scientist, where he leads coupled future antenna projects include transparent antennas. He has authored or coauthored over 40 journal and conference papers and more than 30 patent grants and applications.

Dr. Morimoto received the Young Engineer Award from the IEEE MTT-S Japan Chapter in 2018. He is a member of the Institute of Electronics, Information and Communication Engineers, Japan.

SAM SHIU received the B.Eng. degree from McGill University, Montreal, QC, Canada, the M.Sc. and Ph.D. degrees in mechanical engineering specialized in industrial engineering from the University of Michigan at Ann Arbor, Ann Arbor, MI, USA, and the M.B.A. degree from Ivey Business School, London, ON, Canada. Since 2008, he has been focusing on innovative antenna and its mechanical design in undisclosed new product introductions during his 13.5 years of work tenure with Apple as a Hardware Engineer, and currently as an Antenna Research Scientist with Meta Reality Lab focusing on new technology initiatives. He has authored or coauthored 12 journal and conference papers, more than 36 patent grants, and 15 pending applications. His current research interests include transparent antenna mechanical design for smart glass and augmented reality devices, radar sensing applications, and novel antenna manufacturing processes.

IRENE WEI HUANG (Senior Member, IEEE) received the B.Eng. degree from the China University of Geosciences, Wuhan, China, in 2002, and the M.A.Sc. and Ph.D. degrees in electrical engineering specialized in electromagnetics from the University of Mississippi, Oxford, MS, USA, in 2005 and 2009, respectively. Since 2008, she has been highly focusing on innovative antenna design in research and development of antenna and RF device and system during her work tenure with Nokia, Huawei, and Foxconn Research Department as an Antenna Specialist, a Senior Staff Antenna Engineer, and an Antenna Manager. She is currently an Antenna Research Scientist with Meta Reality Lab. She has authored or coauthored 21 journal and conference papers and more than 20 patent grants and applications. Her current research interests include transparent antenna design for smart glass and augmented reality devices and millimeter-wave antenna in package or antenna in module design for communications and sensing.

ERIC FEST received the Ph.D. degree in optics from the University of Arizona. He is an Optical Scientist with Meta Platforms, Redmond, WA, USA, where he leads the Augmented Reality Product Waveguide Design Team. He is also an Adjunct Associate Professor with the University of Arizona. He has 29 years of experience in the optics industry, and his former employers include Raytheon and Synopsys, Inc. He is the author of the widely used optical engineering textbook *Stray Light Analysis and Control* (SPIE Press, 2013).

GENG YE is the Head of Antenna Engineering with Meta Reality Labs, Sunnyvale, CA, USA. He has been instrumental in creating unique antenna design for Meta's virtual/artificial reality devices.

JIANG ZHU (Fellow, IEEE) received the B.S. degree in information science and electronic engineering from Zhejiang University, China, the M.A.Sc. degree in electrical engineering from McMaster University, Canada, and the Ph.D. degree in electrical engineering from the University of Toronto, Canada.

From 2010 to 2014, he was a Senior Hardware Engineer with Apple Inc., Cupertino, CA, USA. From 2014 to 2016, he was with Google[x] Life Science Division and then a Founding Member with Verily Life Science, a subsidiary of Alphabet Inc., Mountain View. From 2016 to 2021, he founded the Wearable Wireless Hardware Group with Google LLC, Mountain View, CA, USA, and led the antenna and RF research and development for the emerging Wrist-worn, Hearable, Virtual Reality and Augmented Reality products, projects, and technologies. In 2021, he joined Meta Reality Labs, Sunnyvale, CA, USA, as the Head of Antenna Research, where he leads a group of talented and diverse research scientists and engineers working on the enabling technologies for the immersive wearable computing. His work leads to over 100 IEEE journal and conference publications and U.S. patents, many of them have been commercialized in some of the most popular consumer products in the world. His research interests are the consumer applications of RF, antennas, and electromagnetics in the areas of wireless communications, human body interaction and sensing, and wireless power.

Dr. Zhu was a recipient of the IEEE Microwave Theory and Techniques Society Outstanding Young Engineer Award and the IEEE Antennas and Propagation Society Doctoral Research Award. He has received several Student Paper Awards as a student as well as a Project Supervisor, including the most recent one–the First Place Best Student Paper Award in the 2021 IEEE AP-S Symposium on Antennas and Propagation with his Intern Student at Google. He serves as the TPC Chair for the 2023 IEEE International Workshop on Antenna Technology and the TPC Co-Chair for the 2022 IEEE International Microwave Biomedical Conference. He serves on TPC and TPRC for numerous conferences, including IEEE APS, IMS, and RWS. He has been a Senior Editor for the IEEE OPEN JOURNAL OF ANTENNAS AND PROPAGATION and an Associate Editor for the IEEE TRANSACTIONS ON ANTENNAS AND PROPAGATION, the IEEE INTERNET OF THINGS JOURNAL, the IEEE ANTENNAS AND WIRELESS PROPAGATION LETTERS, and *IET Microwaves, Antennas, and Propagation*. He is also the Guest Co-Editor for the *IEEE Communications Magazine*—Special Feature Topic on Antenna Systems for 5G and Beyond, and a Guest Co-Editor for the IEEE OPEN JOURNAL OF ANTENNAS AND PROPAGATION—Special Section on Advances in Antenna Design for Metaverse and Other Modern Smart Mobile Devices. He is a member of the IEEE AP-S Industrial Initiatives Committee and the IEEE AP-S Young Professional Committee, a member and an industry liaison of the IEEE AP-S Membership and Benefits Committee, a member of the IEEE MTT-S Technical Coordination Future Directions Committee—IoT Working Group, and a member of the IEEE MTT-26 RFID, Wireless Sensors, and IoT Committee.